

# Characteristics of particulate-bound *n*-alkanes indicating sources of PM<sub>2.5</sub> in Beijing, China

Jiyuan Yang<sup>1</sup>, Guoyang Lei<sup>1</sup>, Chang Liu<sup>1</sup>, Yutong Wu<sup>1</sup>, Kai Hu<sup>1</sup>, Jinfeng Zhu<sup>1</sup>, Junsong Bao<sup>2</sup>, Weili Lin<sup>1</sup> and Jun Jin<sup>1,3</sup>.

<sup>1</sup>College of Life and Environmental Sciences, Minzu University of China, Beijing 100081, China

<sup>2</sup>State Key Laboratory of Water Environment Simulation, School of Environment, Beijing Normal University, Beijing, 100875, China

<sup>3</sup>Beijing Engineering Research Center of Food Environment and Public Health, Minzu University of China, Beijing 100081, China

Correspondence to: Jun Jin (junjin3799@126.com)

**Abstract.** The characteristics of *n*-alkanes and the contributions of various sources of fine particulate matter (PM<sub>2.5</sub>) in the atmosphere in Beijing were investigated. PM<sub>2.5</sub> samples were collected at Minzu University of China between November 2020 and October 2021, and *n*-alkanes in the samples were analyzed by gas chromatography mass spectrometry. A positive matrix factorization analysis model and source indices (the main carbon peaks, carbon preference indices, and plant wax contribution ratios) were used to identify the sources of *n*-alkanes, determine the contributions of different sources, and explain the differences. The *n*-alkane concentrations were 4.51–153 ng/m<sup>3</sup>, (mean 32.7 ng/m<sup>3</sup>), and the particulate-bound *n*-alkane and PM<sub>2.5</sub> concentrations varied in parallel. There were marked seasonal and diurnal differences in the *n*-alkane concentrations ( $p < 0.01$ ). The *n*-alkane concentrations in the different seasons decreased in the order winter > spring > summer > fall. The mean concentration of each homolog was higher at night than in the day in all seasons. Particulate-bound *n*-alkanes were supplied by common anthropogenic and biogenic sources, and fossil fuel combustion was the dominant contributor. The positive matrix factorization model results indicated five sources of *n*-alkanes in PM<sub>2.5</sub>, which were coal combustion, diesel vehicle emissions, gasoline vehicle emissions, terrestrial plants, and mixed source. Vehicle emissions were the main sources of *n*-alkanes, contributing 57.6%. The sources of PM<sub>2.5</sub> can be indicated by *n*-alkanes (i.e., using *n*-alkanes as organic tracers). Vehicle exhausts strongly affect PM<sub>2.5</sub> pollution. Controlling vehicle exhaust emissions is key to controlling *n*-alkane and PM<sub>2.5</sub> pollution in Beijing.

## 1 Introduction

Serious air pollution in China is currently caused by a combination of haze and photochemical smog (Ma et al., 2012). The effects of haze on air quality are more obvious than the effects of photochemical pollution, which is relatively invisible. Haze is frequent in urban areas with relatively dense populations and high traffic loads. Fine particulate matter is the main pollutant involved in haze. Fine particulate matter has small particle sizes, a long atmospheric retention time, and a complex chemical composition. Fine particulate matter is also a good substrate for chemical reactions, about which there is great concern because the products can negatively affect the environment and human health (Wang et al., 2016; Zhu et al., 2005; Zhang, et al., 2015). In recent years, measures such as energy structure adjustments, pollutant emission controls, and air pollution prevention have markedly decreased atmospheric pollution and improved air quality in China. For example, the PM<sub>2.5</sub> concentration in Beijing, a typical large city in China, has recently decreased markedly. The annual mean PM<sub>2.5</sub> concentration decreased from 73 µg/m<sup>3</sup> in 2016 to 33 µg/m<sup>3</sup> (meeting the requirement of the secondary ambient air quality standard for China, 35 µg/m<sup>3</sup>) in 2021 (Beijing Ecology and Environment Statement, 2016-2021). Sources of fine particulate matter need to be better understood and controlled to decrease PM<sub>2.5</sub> pollution, improve air quality, and meet the primary

39 ambient air quality standard for China ( $15 \mu\text{g}/\text{m}^3$ ) and even the World Health Organization standard ( $5 \mu\text{g}/\text{m}^3$ ).  
40 It has been found that *n*-alkanes are important components of organic pollutants in particulate matter and are mainly supplied  
41 through anthropogenic emissions such as vehicle exhausts, fossil fuel combustion, and biomass combustion (Liu et al., 2013)  
42 or through biogenic emissions such as from microorganisms and terrestrial plants (Simoneit et al., 1989; Rogge et al., 1993).  
43 *n*-Alkanes are non-polar saturated hydrocarbons that are stable and found at high concentrations in the atmosphere. *n*-  
44 Alkanes readily adsorb to particles and can affect the environment and human health (Chen et al., 2019). *n*-Alkanes can  
45 participate in atmospheric chemical reactions, and *n*-alkane volatility and reactivity decrease as the carbon chain length  
46 increases (Aumont et al., 2013). The products of reactions involving short-chain *n*-alkanes ( $C \leq 16$ ) in the environment  
47 strongly contribute to secondary organic aerosol formation (Michoud et al., 2012). Long-chain *n*-alkanes ( $C > 16$ ) are  
48 relatively stable in the environment and generally accumulate in particulate matter (Chrysikou et al., 2009). The carbon  
49 number ranges, molecular compositions, and distributions of *n*-alkane mixtures in particulate matter can be used to assess  
50 aerosol migration and particulate matter sources. Particulate-bound *n*-alkanes play an important role in studying organic  
51 aerosols and the sources of the PM<sub>2.5</sub>. The characteristics and sources of *n*-alkanes in fine particulate matter are important  
52 parameters for developing pollutant control strategies to sustainably decrease haze pollution and improve air quality.  
53 Previous studies of *n*-alkanes in atmospheric particulate matter have mainly been focused on concentrations (Wang et al.,  
54 2005; Wang et al., 2006; Chen et al., 2014; Ren et al., 2017), characteristics (Simoneit et al., 2004; Li et al., 2013; Kang et al.,  
55 2016), and sources (Kavouras et al., 2001; Bi et al., 2003; Fu et al., 2010; Sun et al., 2021). A wide range of *n*-alkanes are  
56 present in the atmosphere, including highly and poorly volatile *n*-alkanes with carbon chain lengths between 8 and 40 (Kang  
57 et al., 2016; Aumont et al., 2012). *n*-Alkane concentrations between tens and hundreds of nanograms per cubic meter have  
58 been found in fine particles (Ren et al., 2016; Lyu et al., 2019). The *n*-alkane concentration is affected by factors such as  
59 meteorological conditions and contributing sources and is related to the particulate matter concentration and particle size  
60 distribution. The total *n*-alkane concentration in particulate matter markedly varies by season, usually being higher in winter  
61 and lowest in summer and fall (Lyu et al., 2016; Chen et al., 2019). *n*-Alkanes from different sources have different  
62 molecular compositions and distributions that can be used to indicate the relative contributions of different sources of  
63 particulate matter (Han et al., 2018).  
64 In the past few decades, researchers in Zhengzhou (Wang et al., 2017), Guangzhou (Bi et al., 2003; Wang et al., 2016),  
65 Shanghai (Lyu et al., 2016; Xu et al., 2015), Beijing (Ren et al., 2016; Lyu et al., 2019), Seoul (Kang et al., 2020), and Spain  
66 (Caumo et al., 2020) have studied *n*-alkanes in atmospheric aerosols and determined total *n*-alkane concentrations, particle  
67 size distributions, and the contributions of different sources. However, *n*-alkanes with different carbon number ranges were  
68 analyzed in the different studies. Most studies were focused on *n*-alkanes containing  $< 30$  carbon atoms, but these do not fully  
69 reflect the sources of *n*-alkanes in particulate matter. Air quality in Beijing is gradually improving, and exploring strategies  
70 for controlling sources of fine particulate matter further requires more information about *n*-alkane homolog distributions and  
71 variability in fine particulate matter and the relative contributions of different sources. Beijing is a large city with a dense  
72 population and high traffic volumes. The sources of *n*-alkanes and particulate matter in Beijing require attention because of  
73 the large number of volatile organic pollutants present, the high levels of vehicle exhaust emissions, and relatively severe  
74 particulate matter pollution. Secondary aerosols have been found to make strong contributions to particulate pollution during  
75 haze episodes in urban areas (Presto et al., 2009; Huang et al., 2014). *n*-Alkanes only contribute a proportion of the total  
76 organic matter in particulate matter but are important contributors to particulate pollution by being important precursors of  
77 secondary organic aerosols (Yang et al., 2019). *n*-Alkanes are also important indicators of the sources of particulate matter.  
78 In this study, the concentrations of C<sub>13</sub>–C<sub>40</sub> *n*-alkanes in atmospheric fine particulate matter in Beijing between 2020 and  
79 2021 were determined. Diurnal and seasonal variations in *n*-alkane homolog concentrations were assessed by performing  
80 diurnal and cross-seasonal sampling. The sources of *n*-alkanes were identified and the contributions of these sources to the  
81 total *n*-alkane concentrations were determined using source indices and correlation models. The aim was to use *n*-alkanes to

82 indicate the sources of particulate matter to allow strategies for controlling particulate matter concentrations in urban areas to  
83 be developed.

## 84 **2 Materials and methods**

### 85 **2.1 Sampling site and time**

86 *Fine particulate matter samples were collected between November 2020 and October 2021* on the roof (about 20 m above the  
87 ground) of the College of Pharmacy at the Minzu University of China (116.19° E, 39.57° N). *Beijing is a typical heavily*  
88 *populated and traffic-intensive Chinese city*, with high emission intensities of nitrogen oxides and volatile organic pollutants  
89 and relatively serious fine particulate matter pollution. Haidian District is a prosperous urban area in Beijing with intense  
90 human activities and busy traffic. The sampling point in Haidian District reflected the influences of human activities and  
91 vehicle emissions on fine particulate matter concentrations. Samples were collected between the 23rd and 29th of each  
92 month during the study, but the exact sampling periods were adjusted to take into account pollution levels and the weather.  
93 Samples were collected in two periods on a sampling day. Daytime samples were collected between 07:00 and 20:00 and  
94 nighttime samples were collected between 20:30 and 06:30 the next morning. Diurnal and seasonal variations in *n*-alkane  
95 concentrations in fine particulate matter were investigated by collecting separate day and night samples and collecting  
96 samples in different seasons. *The effects of n-alkanes on PM2.5 concentrations were assessed by analyzing the correlation*  
97 *between their concentrations.*

### 98 **2.2 Sample collection and pretreatment**

99 Each fine particulate sample was collected using a TH-16A low-flow sampler (Wuhan Tianhong, Wuhan, China) containing  
100 a Whatman QMA quartz fiber filter (Ø 47 mm; GE Healthcare Bio-Sciences, Pittsburgh, PA, USA) using a flow rate of 16.7  
101 L/min. Before use, the quartz fiber filters were baked at 550 °C for 5 h to remove organic matter. Each filter was loosely  
102 wrapped in aluminum foil and equilibrated for 24 h at 20 °C and 40% relative humidity and then weighed using a precision  
103 electronic balance before being used to collect a sample. Once used, a filter was equilibrated for 24 h at 20 °C and 40%  
104 relative humidity, weighed again, and then stored wrapped in aluminum foil at -20 °C.

105 The details for ultrasonic extraction methods used to analyze the samples of *n*-alkanes in PM2.5 are reported in previous  
106 studies (Yang et al., 2019; Kang et al., 2020; Caumo et al., 2020). Each filter was cut into pieces and extracted by  
107 ultrasonically with 15 mL of dichloromethane for 15 min. The extraction step was repeated five times, and the extracts  
108 were combined and evaporated to 2 mL using a rotary evaporator. The extract was then transferred to a 15 mL centrifuge  
109 tube and centrifuged at 3000 rpm for 5 min. The supernatant was evaporated just to dryness under a gentle flow of high  
110 purity nitrogen and then redissolved in 100 µL of toluene for instrumental analysis.

### 111 **2.3 Instrumental analysis**

112 The *n*-alkanes (C<sub>13</sub>–C<sub>40</sub>) were analyzed qualitatively and quantitatively by gas chromatography mass spectrometry using an  
113 Agilent 6890N-5975 system (Agilent Technologies, Santa Clara, CA, USA). *n*-Alkane standards (C<sub>8</sub>–C<sub>40</sub>) were purchased  
114 from AccuStandard (New Haven, CT, USA). Separation was achieved using an Agilent J&W Scientific DB-5M column (30  
115 m long, 0.25 mm inner diameter, 0.1 µm film thickness; Agilent Technologies). *Temperature of the GC inlet was 290°C*,  
116 splitless injection mode was used, and the injection volume was 1.0 µL. The carrier gas was helium and the constant flow  
117 rate was 1.0 mL/min. The oven temperature program started at 80 °C, which was held for 2 min, then increased at 10 °C/min  
118 to 200 °C, and then increased at 15 °C/min to 300 °C, which was held for 30 min. The mass spectrometer was used in  
119 electron impact ionization mode and selected ion detection mode. Ions with mass-to-charge ratios of 85 and 113

120 (characteristic of *n*-alkanes) were used to identify and quantify *n*-alkanes. The data were quantified using ChemStation  
121 software (Agilent Technologies).

## 122 2.4 Quantitative analysis

123 Particulate-bound *n*-alkanes were quantified by external standard method. We prepared standard solutions of C<sub>8</sub>-C<sub>40</sub> *n*-  
124 alkanes with concentration gradients of 10 ppm, 1 ppm, 500 ppb, 100 ppb, 50 ppb and 10 ppb. The calibration curves is  
125 plotted with the concentrations of the standard solution as the abscissa axis and the corresponding chromatographic response  
126 obtained by GC-MS as the ordinate axis, the correlation coefficient of each individual calibration curve is greater than 0.99.  
127 The concentrations of particulate-bound *n*-alkanes were finally quantified by the calibration curves.

## 128 2.5 Quality assurance and control

129 When extracting *n*-alkanes from the fine particulate samples, blank samples were extracted with each batch of samples. The  
130 concentration of an analyte substance in the blanks was subtracted from the concentration of the analyte in a sample during  
131 data processing. The detection and quantification limits of the instrument were defined as three and 10 times the signal-to-  
132 noise ratio, respectively. The instrument detection limits for the *n*-alkanes were 1–10 pg.

133 Spiked recovery experiment was used to evaluate the recovery efficiency of particulate-bound *n*-alkanes. Mixed standard  
134 solution of C<sub>8</sub>-C<sub>40</sub> *n*-alkanes (20 μL, 1 ppm) was added to the blank samples, then the blank samples was pre-treat according  
135 to the same methods and the concentrations of *n*-alkanes was detected by GC-MS. The recovery was calculated based on the  
136 theoretical concentrations of *n*-alkanes standard solution and the measured concentrations of *n*-alkanes in the blank spiked  
137 samples. The blank spiked recovery experiments were repeated three times and the final recovery was averaged over the  
138 three experiments, the extraction recovery for *n*-alkanes range from 43.6% to 128%, the RSD for the concentrations of *n*-  
139 alkanes is 3.51%.

## 140 2.6 Data analysis

141 PM<sub>2.5</sub> data were provided by the China Meteorological Administration (cma.gov.cn). Data analysis (statistical and other  
142 analyses of the *n*-alkane data) was performed using SPSS 26.0 software (IBM, Armonk, NY, USA). Differences in the  
143 concentrations of an *n*-alkane homolog in different groups of samples and differences in the overall *n*-alkane compositions in  
144 different groups of samples were assessed by performing independent sample t-tests. Spearman correlations and Pearson  
145 correlations (two-tailed tests) were used to identify correlations between groups of data.

146 Source indices (the carbon maximum number (C<sub>max</sub>), carbon preference index (CPI), and plant wax *n*-alkane ratio  
147 (WNA%)) were used to assess the *n*-alkane sources from the *n*-alkane molecular compositions and concentration  
148 distributions. The C<sub>max</sub> is the homolog with the highest relative concentration in the *n*-alkane mixture, it is commonly used  
149 to distinguish between the contributions of anthropogenic and natural sources of *n*-alkanes and is related to the degree of  
150 thermal evolution that has affected the organic matter supplying *n*-alkanes. The CPI defined as the ratio of total odd carbon  
151 *n*-alkanes to even carbon *n*-alkanes and was developed by Bray and Evans in 1961 (Bray et al., 1961), it can be used to  
152 assess the contributions of anthropogenic and biogenic sources of *n*-alkanes and is the most commonly used empirical  
153 parameter for distinguishing between sources of *n*-alkanes (Marzi et al., 1993). WNA% and PNA% (petrogenic *n*-alkane  
154 ratio) can be used to assess the relative contributions of biological and anthropogenic sources of *n*-alkanes in particulate  
155 matter (Simoneit, 1985), WNA% are calculated by subtraction of the average of the next higher and lower even carbon  
156 numbered homologues, while PNA% was defined as the WNA% subtracted from 100% (Lyu et al., 2019). The source  
157 indices were calculated using Eqs. (1)–(3):

$$158 \quad \text{CPI} = \frac{\sum_{i=6}^{19} C_{2i+1}}{\sum_{i=7}^{20} C_{2i}} \quad (1)$$

$$159 \quad \text{WNA}\% = \frac{\sum (C_n - (\frac{C_{n-1} + C_{n+1}}{2}))}{\sum C_n} \times 100\% \text{ ("n" is an odd number)} \quad (2)$$

$$160 \quad \text{PNA}\% = 100\% - \text{WNA}\% \quad (3)$$

161 In Eq. (1),  $C_{2i+1}$  was the concentration of the  $n$ -alkane with odd carbon atoms range from 13-39, while  $C_{2i}$  was the  
 162 concentration of the  $n$ -alkane with even carbon atoms range from 14-40. In Eq. (2),  $C_n$  was the concentration of  $n$ -alkanes,  
 163 taking as zero the negative value of  $(C_n - (\frac{C_{n-1} + C_{n+1}}{2}))$ .

164 A positive matrix factorization (PMF) model was used to identify specific  $n$ -alkane sources and the contribution of each  
 165 source through EPA PMF 5.0 software (USEPA). The PMF model is a factor analysis technique using multivariate statistical  
 166 methods. The PMF model is a receptor model, so can identify and determine the contributions of components of unknown  
 167 mixtures. The PMF model is one of the source resolution methods recommended by the US Environmental Protection  
 168 Agency. The PMF model does not require the complex pollutant sources to be determined and the treatment process can be  
 169 optimized while limiting the decomposition matrix elements and sharing the rates of nonnegative matrices. The model can  
 170 use the chemical composition of particulate matter to identify the sources of particulate matter and calculate the contributions  
 171 of the different sources, so is widely used to investigate the sources of atmospheric particulate matter (Moeinaddini et al.,  
 172 2014; Liao et al., 2021; Li et al., 2021). The details of PMF have been described in the PMF 5.0 User Guide (USEPA, 2014).

## 173 **3 Results**

### 174 **3.1 Concentrations of $n$ -alkanes**

175 A total of 28  $n$ -alkane homologs with carbon chain lengths of  $C_{13}$ – $C_{40}$  were analyzed.  $C_{13}$ – $C_{40}$   $n$ -alkanes were detected in the  
 176 diurnal fine particulate matter samples collected in all seasons. Among them,  $C_{21}$ – $C_{35}$   $n$ -alkanes were detected in all PM2.5  
 177 samples, other  $n$ -alkanes were detected in more than half of the samples.

178 *The  $n$ -alkane and PM2.5 concentrations in the different seasons are shown in Table 1 and temporal variations in the average  
 179 concentrations between day and night are shown in Figure 1. The PM2.5 concentrations throughout the sampling period were  
 180 0–134  $\mu\text{g}/\text{m}^3$ , and the mean was 32.0  $\mu\text{g}/\text{m}^3$ . The  $n$ -alkane concentrations throughout the sampling period were 4.51–153  
 181  $\text{ng}/\text{m}^3$ , and the mean was 32.7  $\text{ng}/\text{m}^3$ . As shown in Figure 8, under the condition of excluding the influence of the sharp rise  
 182 of PM2.5 concentration in heavy haze days, correlation analysis indicated that the  $n$ -alkane and PM2.5 concentrations  
 183 significantly positively correlated ( $p < 0.01$ ,  $r = 0.618$ ).*

### 184 **3.2 $n$ -Alkane component distributions**

185 The contributions of the individual  $C_{13}$ – $C_{40}$   $n$ -alkane homologs to the total  $n$ -alkane concentrations are shown in Figure 2.  
 186 The  $C_{16}$ – $C_{25}$   $n$ -alkanes were dominant in winter and the  $C_{26}$ – $C_{31}$   $n$ -alkane contributions increased markedly spring, summer,  
 187 and fall.

188 The  $n$ -alkane homologs can be classed as low molecular weight (LMW), meaning  $n$ -alkanes with carbon chain lengths  $\leq 25$ ,  
 189 and high molecular weight (HMW), meaning  $n$ -alkanes with carbon chain lengths  $> 25$ . As shown in Figure 3, LMW  $n$ -  
 190 alkanes contributed  $\sim 60\%$  of the total  $n$ -alkane concentrations in winter but only  $\sim 40\%$  in spring, summer, and fall,  
 191 indicating that there were marked differences between the compositions in winter and the other seasons.

### 192 3.3 Seasonal and diurnal differences in *n*-alkane concentrations

193 The average concentration distributions of C<sub>13</sub>–C<sub>40</sub> *n*-alkanes in the different seasons are shown in Figure 4. There were  
194 significant differences ( $p < 0.01$ ) between the concentrations of various homologs in the different seasons. The mean *n*-alkane  
195 concentrations for the different seasons decreased in the order winter > spring > summer > fall. The seasonal differences were  
196 more marked for LMW than HMW *n*-alkanes. The concentrations of relatively short-chain *n*-alkanes (C<sub>16</sub>–C<sub>25</sub>) were  
197 markedly higher in winter than in the other seasons. The concentrations of C<sub>27</sub>, C<sub>29</sub>, C<sub>31</sub>, and C<sub>33</sub> *n*-alkanes were higher than  
198 the concentrations of C<sub>26</sub>, C<sub>28</sub>, C<sub>30</sub>, C<sub>32</sub>, and C<sub>34</sub> *n*-alkanes (i.e., odd-carbon-number dominance occurred) in all of the seasons.  
199 The C<sub>13</sub>–C<sub>40</sub> *n*-alkane concentrations in the day and night samples are shown in Figure 5. The mean *n*-alkane homolog  
200 concentrations were higher at night than in the day in all four seasons. The concentrations in the day and night were  
201 significantly different ( $p < 0.01$ ). Statistical tests on the differences in concentration of individual homolog of *n*-alkanes  
202 between day and night in different seasons showed that fewer *n*-alkane homologs with significant differences in winter (C<sub>16</sub>,  
203 C<sub>17</sub>) and spring (C<sub>21</sub>) while more *n*-alkane homologs (C > 21) with significant differences in summer and autumn.

### 204 3.4 Source indices and PMF model

205 Source indices (C<sub>max</sub>, CPI, and WNA%) determined from the C<sub>13</sub>–C<sub>40</sub> *n*-alkane data were used to assess the *n*-alkane  
206 sources. The PMF model was used to quantify the amounts of *n*-alkanes in fine particles supplied by the different sources  
207 and the relative contributions of the sources. The source index data for *n*-alkanes in the day and night samples in the different  
208 seasons are shown in Table 2.

#### 209 3.4.1 Source indices for *n*-alkanes

210 The C<sub>max</sub> for winter was C<sub>23</sub> but the C<sub>max</sub> for spring, summer, and fall was C<sub>29</sub>. The mean CPI for the year the samples  
211 were collected were 1.66. The CPI was lowest in winter but higher in the day than the night in spring, summer, and fall. The  
212 mean contribution of plant wax *n*-alkanes to the total *n*-alkane concentration during the sampling period was 30.6% and the  
213 mean contribution of anthropogenic *n*-alkanes to the total *n*-alkane concentration was 69.4%. The plant wax *n*-alkane  
214 contribution was lowest in winter and markedly higher in spring, summer, and fall.

#### 215 3.4.2 Results of the PMF model

216 According to the PMF 5.0 User Guide (USEPA, 2014), the daily mean *n*-alkane concentrations during the sampling period  
217 and the corresponding uncertainties were inputted into the PMF model to analyze the sources of *n*-alkanes in fine particulate  
218 matter. Various numbers of factors were tested, and the optimal correlation coefficient for the relationship between the  
219 simulated and observed values was found when five factors were used, the average correlation coefficient of *n*-alkane  
220 homologues is 0.832. Q (robust) is a important parameter obtained after PMF run, it is the goodness-of-fit parameter  
221 calculated excluding points not fit by the model (USEPA, 2014). In the process of running the PMF model, we got the lowest  
222 Q (robust) values when selected five factors. This met the requirements to use the PMF model, EPA PMF 5.0 User Guide  
223 (USEPA, 2014) have stated that the lowest Q (robust) value represents the most optimal solution from the multiple runs and  
224 it can be a critical parameter for choosing optimal number of factors. Each factor indicated a source, and the factors could be  
225 used to identify the corresponding sources. The *n*-alkane factor data given by the PMF model are shown in Figure 6.  
226 The PMF model indicated that the contributions of factors 1, 2, 3, 4, and 5 to the *n*-alkane concentrations were 14.8%, 26.1%,  
227 31.5%, 18.6%, and 9.01%, respectively. The sources corresponding to the factors identified by the PMF model needed to be  
228 identified from the proportions of the different *n*-alkane homologs present, the sources corresponding to factors 2 and 3 were  
229 the main contributors of *n*-alkanes in particulate matter.

231 **4.1 Sources and contributions of *n*-alkanes**

232 *n*-Alkanes in PM<sub>2.5</sub> have relatively complex sources, but different *n*-alkane compositions and distributions indicate different  
233 sources. As shown in Figure 4, marked odd-carbon-number dominance was found in all seasons for the HMW *n*-alkanes,  
234 with *n*-alkanes with carbon chain lengths C<sub>27</sub>, C<sub>29</sub>, C<sub>31</sub>, and C<sub>33</sub> being dominant. No odd-carbon-number dominance was  
235 found for the LMW *n*-alkanes. It has previously been found that LMW *n*-alkanes in urban areas are mainly anthropogenic  
236 (e.g., emitted during fossil fuel combustion and in vehicle exhaust gases) (Simoneit et al., 2004; Kang et al., 2016) but HMW  
237 *n*-alkanes reflect sources such as biomass combustion and waxes in terrestrial plants (Kawamura et al., 2003). LMW and  
238 HMW *n*-alkane patterns can be used to identify the main sources of *n*-alkanes in urban areas. The *n*-alkane patterns in the  
239 different seasons indicated that particulate-bound *n*-alkanes in the atmosphere in Beijing have both anthropogenic and  
240 biological sources. The source indices and PMF model results further explained the sources and contributions of *n*-alkanes.

241 *n*-Alkane source indices are often used to identify the origins of *n*-alkanes. The *n*-alkane source indices shown in Table 2  
242 indicated that anthropogenic emissions were the main contributors of particulate-bound *n*-alkanes in Beijing during the study  
243 but that there were also biogenic emissions of particulate-bound *n*-alkanes. The CPI and WNA% data explained this. During  
244 the sampling period, the mean CPI was 1.66, indicating that the main sources of particulate-bound *n*-alkanes were fossil fuel  
245 combustion, plants, and biomass combustion. The mean WNA% and PNA% were 30.63% and 69.37%, respectively,  
246 indicating that anthropogenic emissions contributed more than emissions from biota.

247 The PMF model can quantify the contributions of specific sources of *n*-alkanes relatively accurately. The *n*-alkane homolog  
248 contributions to each factor identified by the PMF model were used to analyze and identify the corresponding source. As  
249 shown in factor 1 of Figure 6, the *n*-alkanes with carbon chain lengths of C<sub>13</sub>–C<sub>18</sub> were dominant, which similar to the *n*-  
250 alkane homolog (C<20) pattern for emissions during coal combustion found by Oros and Simoneit and Niu et al. (Oros et al.,  
251 2000; Niu et al., 2005). Therefore, we concluded that factor 1 indicated *n*-alkanes emitted through coal combustion. Vehicle  
252 emissions are important sources of *n*-alkanes in particulate matter in urban areas (Lyu et al., 2019). *n*-Alkanes emitted by  
253 vehicles mainly have carbon-chain lengths <30 (Wang et al., 2017). However, there are marked differences between the  
254 patterns of *n*-alkanes emitted in particulates in gasoline vehicle and diesel vehicle exhaust gases. C<sub>max</sub> for *n*-alkanes is lower  
255 and the proportion of low-carbon-chain length *n*-alkanes is higher for particulates in diesel vehicle exhaust gases than  
256 gasoline vehicle exhaust gases. This feature can be used to distinguish between *n*-alkanes emitted by diesel and gasoline  
257 vehicles in fine particulate matter (Fujitani et al., 2012; Yuan et al., 2016). As shown in Figure 6, the homologs with a higher  
258 proportion of *n*-alkane species in factor 2 are concentrated around C<sub>20</sub>, while in factor 3 are concentrated around C<sub>27</sub>.  
259 According to studies of Schauer et al. for gasoline and diesel vehicle emissions (Schauer et al., 1999; Schauer et al., 2002),  
260 we determine that factor 2 and factor 3 indicated diesel and gasoline vehicle emission sources, respectively. C<sub>27</sub>–C<sub>38</sub> (i.e.,  
261 high-carbon-chain-length) *n*-alkanes made large contributions and low-carbon-chain-length *n*-alkanes made small  
262 contributions to the pattern for factor 4. Studies have shown that C<sub>26</sub>–C<sub>36</sub> *n*-alkanes are mainly emitted from cuticular waxes  
263 in terrestrial plants (Alves et al., 2001; Lyu et al., 2016), so we inferred that factor 4 indicated *n*-alkanes emitted by terrestrial  
264 plants. *n*-Alkanes do not have an obvious regularity in composition and there was no clear *n*-alkane homologs pattern for  
265 factor 5, but long-chain *n*-alkanes with carbon chain lengths ≥34 were dominant. We found that road dust is one of the  
266 sources of particulate-bound *n*-alkanes (Anh et al., 2019), *n*-alkanes with ≥C<sub>34</sub> may come from road dust (Daher et al., 2013)  
267 and biogenic source (Liebezeit et al., 2009). Therefore, we concluded that factor 5 may be a mixed source of *n*-alkanes from  
268 road dust and biogenic emissions.

269 The contributions of the different sources to the *n*-alkane concentrations are shown in Figure 7. In summary, *n*-alkanes in  
270 airborne particulate matter in Beijing are both anthropogenic and biogenic. Vehicle exhaust emissions are the main sources  
271 of *n*-alkanes, consistent with the current energy consumption structure in Beijing, and gasoline and diesel vehicles accounted

272 for a relatively large proportion of *n*-alkanes in airborne particulate matter.

## 273 **4.2 Characteristics of PM<sub>2.5</sub> and *n*-alkanes**

274 The mean *n*-alkane concentration during the sampling period was 32.7 ng/m<sup>3</sup>, which was lower than the C<sub>19</sub>–C<sub>36</sub> *n*-alkane  
275 concentration of 282 ng/m<sup>3</sup> found in Beijing in 2006 (Li et al., 2013) and the C<sub>8</sub>–C<sub>40</sub> *n*-alkane concentration of 228 ng/m<sup>3</sup>  
276 found in Shanghai in 2013 (Lyu et al., 2016). The temporal trends in the *n*-alkane concentrations were similar to the trends  
277 found in previous studies of *n*-alkanes in Beijing (Rogge et al., 1993; Li et al., 2013; Ren et al., 2019), the overall *n*-alkane  
278 concentration being highest in winter. The seasonal pattern we found for *n*-alkanes in Beijing was similar to the pattern  
279 found in a previous study of C<sub>16</sub>–C<sub>35</sub> *n*-alkanes in 14 Chinese cities (Wang et al., 2006).

280 The *n*-alkane pattern varied by season, LMW *n*-alkanes being dominant in winter and HMW *n*-alkanes being more abundant  
281 in the other seasons. C<sub>max</sub> and WNA% explained the seasonal differences in the *n*-alkane patterns. In previous studies,  
282 lower C<sub>max</sub> values were found for *n*-alkanes emitted from very mature organic matter such as coal and petroleum than for *n*-  
283 alkanes emitted from immature organic matter such as plants (Simoneit et al., 1989; Duan et al., 2010). The C<sub>max</sub> for *n*-  
284 alkanes in winter was C<sub>23</sub>, indicating that LMW *n*-alkanes were the main *n*-alkanes. Similar results were found by Lyu et al.  
285 for Beijing in winter (Lyu et al., 2019). The C<sub>max</sub> for *n*-alkanes in spring, summer, and fall was C<sub>29</sub>. Ficken et al. (Ficken et  
286 al., 2000) and Yadav et al. (Yadav et al., 2013) found that C<sub>29</sub> *n*-alkanes are markers for *n*-alkanes emitted from the wax  
287 layers of terrestrial plants. Stronger *n*-alkane contributions will be made by plants in spring, summer, and fall than in winter  
288 (Rogge et al., 1993; Yadav et al., 2013). This is consistent with the results found in a study performed in Shanghai (Lyu et al.,  
289 2016; Wang et al., 2016). There were significant seasonal differences ( $p < 0.01$ ) in the concentrations of the C<sub>13</sub>–C<sub>40</sub> *n*-alkane  
290 homologs, but the seasonal differences were stronger for LMW *n*-alkanes than HMW *n*-alkanes. Similar results were found  
291 by Li et al. in Tianjin in 2010 (Li et al., 2010). The LMW *n*-alkane concentrations were markedly higher in winter than in the  
292 other seasons, similar to the results of a study performed by Li et al. in Beijing in 2013 (Li et al., 2013). This indicated that  
293 there were seasonal differences in *n*-alkane sources. The PMF model results shown in Figure 7 indicated that anthropogenic  
294 *n*-alkanes strongly contributed to the total *n*-alkane concentration in winter. The CPI also indicated that different sources  
295 were dominant in winter and in the other seasons. The lowest CPI was found for winter, indicating that LMW *n*-alkanes  
296 made stronger contributions to the total *n*-alkane concentrations in winter than the other seasons. This may be related to *n*-  
297 alkane emissions caused by fossil fuel combustion for heating in winter. Similar results have been found in Shanghai (Lyu et  
298 al., 2016), Zhengzhou (Wang et al., 2017), southeastern Chinese cities (Chen et al., 2019), and Beijing (Kang et al., 2016).

299 *Meteorological factors affect the concentrations and composition of *n*-alkanes in different seasons. The mixing layer height*  
300 *influences the concentration of *n*-alkanes by affecting the particulate matter, it's shown that the mixing layer height is*  
301 *correlated with the concentration of particulate matter and the peak concentration of particulate matter increases as the*  
302 *mixing layer height decreases (Wagner et al., 2017). The atmospheric mixing layer height in Beijing has obvious seasonal*  
303 *characteristics, showing low in winter and high in summer (Wang et al., 2020; Tang et al., 2016). Therefore, the increased*  
304 *concentrations of PM<sub>2.5</sub> and *n*-alkanes in winter were influenced by the mixing layer height. Wind direction is one of the*  
305 *factors affecting the seasonal differences in particulate matter and *n*-alkanes, the northwest wind in winter brought the*  
306 *polluted air masses from inland to Beijing, while the southeast wind in summer transported cleaner aerosols from oceans to*  
307 *here (Wei et al., 2020). In addition, the seasonal distribution of *n*-alkanes is influenced by the temperature. The temperature*  
308 *in Beijing is high in summer and low in winter, when the temperature is lower in winter, gaseous *n*-alkanes are more likely to*  
309 *partition into particles with the higher partition coefficient of gas-particle partitioning (Lyu et al., 2016; Wick et al., 2002).*  
310 *Therefore, the increase of LWM *n*-alkanes proportion in winter also affected by temperature.*

311 The mean C<sub>13</sub>–C<sub>40</sub> *n*-alkane homolog concentrations were higher at night than in the day in each season, and the differences  
312 were significant ( $p < 0.01$ ). According to the study by Yao et al. in 2009, lower average wind speeds, atmospheric mixing



313 layer height and poorer atmospheric diffusion conditions can lead to higher concentrations of *n*-alkanes at night than in the  
314 day (Yao et al., 2009). Similar results were found in Liaocheng, Shandong Province (Liu et al., 2019). The differences in the  
315 *n*-alkane concentrations in the night and day may also have been caused by differences in pollutant emissions in the night  
316 and day. Particulate-bound *n*-alkanes from vehicular emissions usually of low molecular weight (Lyu et al., 2019), diesel  
317 emissions have higher concentrations of particulate-bound *n*-alkanes with carbon chain lengths less than 25 (Schauer et al.,  
318 1999). Differences in diurnal concentrations of LMW *n*-alkanes may reflect the differences in the contribution of  
319 anthropogenic sources. We found markedly higher concentrations of some homologs with carbon chain lengths <25 at night  
320 than during the day. This would be consistent with short-chain alkane emissions from diesel vehicles in Beijing being higher  
321 at night than in the day.

#### 322 **4.3 PM<sub>2.5</sub> sources in Beijing and strategies for controlling PM<sub>2.5</sub> concentrations**

323 During the sampling period, the mean daily PM<sub>2.5</sub> concentration in Beijing was 32.0 µg/m<sup>3</sup>, which met the requirement of  
324 the secondary ambient air quality standard for China (35.0 µg/m<sup>3</sup>). According to the Ecology and Environment Statement  
325 from the Beijing Municipal Ecology and Environment Bureau (sthjj.beijing.gov.cn), the annual mean PM<sub>2.5</sub> concentration in  
326 Beijing has gradually decreased in the last five years. However, little research on *n*-alkanes in Beijing has been performed in  
327 this period. We compared our results with the results of a previous study (Lyu et al., 2019) and found that the *n*-alkane  
328 concentrations decreased in parallel with the PM<sub>2.5</sub> concentrations. *n*-Alkanes are important molecular markers for  
329 identifying the sources of PM<sub>2.5</sub>. Excluding when the PM<sub>2.5</sub> concentration increased sharply because of meteorological  
330 conditions, the PM<sub>2.5</sub> and *n*-alkane concentrations varied in the same ways. As shown in Figure 8, a significant positive  
331 correlation was found between the PM<sub>2.5</sub> and *n*-alkane concentrations ( $p < 0.01$ ), so *n*-alkanes could be used as indicators of  
332 the sources of PM<sub>2.5</sub> in the atmosphere. This method has been widely used to analyze sources of particulate matter (Cass,  
333 1998; Kavouras et al., 2001; Bi et al., 2003; Xu et al., 2013; Zhao et al., 2016; Han et al., 2018). We therefore used the PMF  
334 model results for *n*-alkanes to identify the sources of PM<sub>2.5</sub> and explain variations in the sources.

335 The PMF model results for the contributions of the different sources shown in Figure 7 indicated that emissions in vehicle  
336 exhaust gases and through coal combustion contributed up to 72.4% of PM<sub>2.5</sub> in the sampling area throughout the sampling  
337 period. This indicated that anthropogenic PM<sub>2.5</sub> emissions are the main sources of PM<sub>2.5</sub> in the urban study area. Emissions  
338 from gasoline and diesel vehicles were the dominant anthropogenic sources, contributing 57.6% of total anthropogenic  
339 PM<sub>2.5</sub> emissions. Vehicles are the main sources of PM<sub>2.5</sub> in urban areas and make important contributions to particulate  
340 matter in the atmosphere in Beijing. Similar results were found in a previous study of PM<sub>2.5</sub> sources in Beijing (Lv et al.,  
341 2020; Qi et al., 2018) and the results were consistent with the current energy consumption structure in Beijing (gasoline and  
342 diesel fuel make large contributions to total fuel consumption). Human activities make larger contributions to PM<sub>2.5</sub>  
343 emissions in winter than the other seasons, indicating that more attention should be paid to emissions caused by fossil fuel  
344 combustion in winter than the other seasons.

345 It is necessary to improve air quality in Beijing, and vehicle exhausts are key sources of PM<sub>2.5</sub>. Further improvements in  
346 ambient air quality to meet stricter ambient air quality standards will require vehicle emissions to be controlled to decrease  
347 particulate matter pollution. The number of vehicles using fossil fuels in Beijing needs to be decreased. Achieving this will  
348 require policies for restricting the use of vehicles using fossil fuels and the use of cleaner energy vehicles to be promoted. In  
349 summary, controlling and decreasing emissions caused by fossil fuel combustion will decrease PM<sub>2.5</sub> emissions and  
350 improve ambient air quality in Beijing.

## 351 **5 Conclusions**

352 The PM<sub>2.5</sub> concentrations and C<sub>13</sub>–C<sub>40</sub> *n*-alkane concentrations in fine particulate matter between November 2020 and  
353 October 2021 were determined and the concentrations were compared with concentrations found in previous studies. The  
354 PM<sub>2.5</sub> and *n*-alkane concentrations in Beijing have decreased in similar ways in the last five years. The mean PM<sub>2.5</sub>  
355 concentration was 32.0 µg/m<sup>3</sup>, which met the secondary ambient air quality standard for China. The PM<sub>2.5</sub> and C<sub>13</sub>–C<sub>40</sub> *n*-  
356 alkane concentrations varied in similar ways and positively correlated ( $p < 0.01$ ), so long chain *n*-alkanes in particulate matter  
357 can be used to assess the sources of particulate matter pollution in urban areas and to develop strategies for controlling  
358 particulate matter pollution.

359 The *n*-alkane concentrations in the different seasons decreased in the order winter>spring>summer>fall. There were marked  
360 seasonal and diurnal differences in the *n*-alkane homolog patterns and distributions. The source indices and PMF model  
361 results explained these variations in patterns and allowed the sources of *n*-alkanes to be identified. The source indices  
362 indicated that *n*-alkane concentrations in particulate matter in Beijing are affected by both anthropogenic and biogenic  
363 emissions but that anthropogenic emissions are dominant. The PMF model allowed the contributions of the sources of *n*-  
364 alkanes to be quantified and indicated that emissions from vehicles are currently the main sources of PM<sub>2.5</sub> and *n*-alkanes in  
365 particulate matter in urban areas.

366 Controlling PM<sub>2.5</sub> and *n*-alkanes emissions from vehicles is key to decreasing PM<sub>2.5</sub> and *n*-alkanes pollution and improving  
367 air quality in urban areas. *n*-Alkanes in particulate matter can be used as organic tracers, and PMF model results can indicate  
368 the sources of PM<sub>2.5</sub> pollution. Further research into the use of this method is required.

## 369 **Acknowledgements**

370 This work was supported by the National Natural Science Foundation of China [grant no. 91744206] and the Beijing Science  
371 and Technology Planning Project [Z181100005418016]. We also thank Dr. Gareth Thomas for his help in grammatical  
372 editing of this paper.

## 373 **Data availability**

374 The data presented in this article are available from the authors upon request (junjin3799@126.com).

## 375 **Author contribution**

376 JJ conceived and designed the study, provided direct funding and helped with manuscript revision. JYY mainly conducted  
377 the sampling, sample analysis work, as well as manuscript writing and revision. Other authors helped this work by sampling  
378 and analysis. All authors read and approved the final manuscript.

## 379 **Competing interests**

380 The authors declare that they have no conflict of interest.

## 381 **References**

382 Alves, C., Pio, C., and Duarte, A.: Composition of extractable organic matter of air particles from rural and urban Portuguese

383 areas, *Atmos. Environ.*, 35, 5485-5496, doi: 10.1016/S1352-2310(01)00243-6, 2001.

384 Aumont, B., Valorso, R., Mouchel-Vallon, C., Camredon, M., Lee-Taylor, J., and Madronich, S.: Modeling SOA formation  
385 from the oxidation of intermediate volatility n-alkanes, *Atmos. Chem. Phys.*, 12, 7577-7589, doi: 10.5194/acp-12-7577-2012,  
386 2012.

387 Aumont, B., Camredon, M., Mouchel-Vallon, C., La, S., Ouzebidour, F., Valorso, R., Lee-Taylor, J., and Madronich, S.:  
388 Modeling the influence of alkane molecular structure on secondary organic aerosol formation, *Faraday Discuss.*, 165, 105-  
389 122, doi: 10.1039/C3FD00029J, 2013.

390 Beijing Ecology and Environment Statement. sthjj.beijing.gov.cn, Beijing Municipal Ecology and Environmental Bureau,  
391 2016-2021.

392 Bi, X. H., Sheng, G. Y., Peng, P. A. Chen, Y. J., Zhang, Z. Q., and Fu, J. M.: Distribution of particulate- and vapor-phase n-  
393 alkanes and polycyclic aromatic hydrocarbons in urban atmosphere of Guangzhou, China, *Atmos. Environ.*, 37, 289-298, doi:  
394 10.1016/S1352-2310(02)00832-4, 2003.

395 Bray, E. E., and Evans, E. D.: Distribution of n-paraffins as a clue to recognition of source beds, *Geochim. Cosmochim.*  
396 *Acta.*, 22, 2-15, doi: 10.1016/0016-7037(61)90069-2, 1961.

397 Cass, G. R.: Organic molecular tracers for particulate air pollution sources, *Trends Analyt. Chem.*, 17, 356-366, doi:  
398 10.1016/S0165-9936(98)00040-5, 1998.

399 Caumo, S., Bruns, R. E., and Vasconcellos, P. C.: Variation of the Distribution of Atmospheric n-Alkanes Emitted by  
400 Different Fuels' Combustion, *Atmosphere*, 11, 643, doi: 10.3390/atmos11060643, 2020.

401 Chen, Q., Chen, Y., Luo, X. S., Hong, Y. W., Hong, Z. Y., Zhao, Z., and Chen, J. S.: Seasonal characteristics and health risks  
402 of PM<sub>2.5</sub>-bound organic pollutants in industrial and urban areas of a China megacity, *J. Environ. Manage.*, 245, 273-281, doi:  
403 10.1016/j.jenvman.2019.05.061, 2019.

404 Chen, Y., Cao, J. J., Zhao, J., Xu, H. M., Arimoto, R., Wang, G. H., Han, Y. M., Shen, Z. X., and Li, G. H.: n-Alkanes and  
405 polycyclic aromatic hydrocarbons in total suspended particulates from the southeastern Tibetan Plateau: concentrations,  
406 seasonal variations, and sources, *Sci. Total Environ.*, 470-471, 9-18, doi: 10.1016/j.scitotenv.2013.09.033, 2014.

407 Chrysikou, L. P., and Samara, C. A.: Seasonal variation of the size distribution of urban particulate matter and associated  
408 organic pollutants in the ambient air, *Atmospheric Environ.*, 43, 4557-4569, doi: 10.1016/j.atmosenv.2009.06.033, 2009.

409 Duan, F. K., He, K. B., and Liu, X. D.: Characteristics and source identification of fine particulate n-alkanes in Beijing,  
410 China, *J. Environ. Sci. (in Chinese)*, 22, 998-1005, doi: 10.1016/S1001-0742(09)60210-2, 2010.

411 Ficken, K. J., Li, B., Swain, D. L., and Eglinton, G.: An n-alkane proxy for the sedimentary input of submerged/floating  
412 freshwater aquatic macrophytes, *Org. Geochem.*, 31, 745-749, [https://doi.org/10.1016/S0146-6380\(00\)00081-4](https://doi.org/10.1016/S0146-6380(00)00081-4), 2000.

413 Fu, P. Q., Kawamura, K., Pavuluri, C. M., Swaminathan, T., and Chen, J.: Molecular characterization of urban organic  
414 aerosol in tropical India: contributions of primary emissions and secondary photooxidation, *Atmos. Chem. Phys.*, 10, 2663-  
415 2689, doi: 10.5194/acp-10-2663-2010, 2010.

416 Fujitani, Y., Saitoh, K., Fushimi, A., Takahashi, K., Hasegawa, S., Tanabe, K., Kobayashi, S., Furuyama, A., Hirano, S., and  
417 Takami, A.: Effect of isothermal dilution on emission factors of organic carbon and n-alkanes in the particle and gas phases  
418 of diesel exhaust, *Atmos. Environ.*, 59, 389-397, doi: 10.1016/j.atmosenv.2012.06.010, 2012.

419 Han, D. M., Fu, Q. Y., Gao, S., Li, L., Ma, Y. G., Qiao, L. P., Xu, H., Liang, S., Cheng, P. F., Chen, X. J., Zhou, Y., Yu, J. Z.,  
420 and Chen, J. P.: Non-polar organic compounds in autumn and winter aerosols in a typical city of eastern China: size  
421 distribution and impact of gas-particle partitioning on PM<sub>2.5</sub> source apportionment, *Atmos. Chem. Phys.*, 18, 9375-9391, doi:  
422 10.5194/acp-18-9375-2018, 2018.

423 Huang, R. J., Zhang, Y. L., Bozzetti, C., Ho, K. F., Cao, J. J., Han, Y. M., Daellenbach, R. K., Slowik, J. G., Platt, S. M.,  
424 Canonaco, F., Zotter, P., Wolf, R., Pieber, S. M., Bruns, E. A., Crippa, M., Ciarelli, G., Piazzalunga, A., Schwikowski, M.,  
425 Abbaszade, G., Schnelle-Kreis, J., Zimmermann, R., An, Z. S., Szidat, S., Baltensperger, U., Haddad, I. E., and Prévôt, A. S

426 H: High secondary aerosol contribution to particulate pollution during haze events in China, *Nature*, 514, 218-222, doi:  
427 10.1038/nature13774, 2014.

428 Kang, M. J., Fu P. Q., Aggarwal, S. G, Kumar, S., Zhao, Y., Sun, Y. L., and Wang, Z. F.: Size distributions of n-alkanes, fatty  
429 acids and fatty alcohols in springtime aerosols from New Delhi, India, *Environ. Pollut.*, 219, 957-966, doi:  
430 10.1016/j.envpol.2016.09.077, 2016.

431 Kang, M. J., Ren, L. J., Ren, H., Zhao, Y., Kawamura, K., Zhang, H. L., Wei, L. F., Sun, Y. L., Wang, Z. F., and Fu, P. Q.:  
432 Primary biogenic and anthropogenic sources of organic aerosols in Beijing, China: Insights from saccharides and n-alkanes,  
433 *Environ. Pollut.*, 243, 1579-1587, doi: 10.1016/j.envpol.2018.09.118, 2016.

434 Kang, M., Kim, K., Choi, N., Kim, Y. P., and Lee, J. Y.: Recent Occurrence of PAHs and n-Alkanes in PM<sub>2.5</sub> in Seoul,  
435 Korea and Characteristics of Their Sources and Toxicity, *Int. J. Environ. Res. Public Health*, 17, 1397, doi:  
436 10.3390/ijerph17041397, 2020.

437 Kavouras, I. G, Koutrakis, P., Tsapakis, M., Lagoudaki, E., Stephanou, E. G, Baer, D. V., and Oyola, P.: Source  
438 apportionment of urban particulate aliphatic and polynuclear aromatic hydrocarbons (PAHs) using multivariate methods,  
439 *Environ. Sci. Technol.*, 35, 2288-2294, doi: 10.1021/es001540z, 2001.

440 Kawamura, K., Ishimura, Y., and Yamazaki, K.: Four years' observations of terrestrial lipid class compounds in marine  
441 aerosols from the western North Pacific, *Global Biogeochem Cycles*, 17, 1-19, doi: 10.1029/2001GB001810, 2003.

442 Li, F. X., Gu, J. W., Xin, J. Y., Schnelle-Kreis, J., Wang, Y. S., Liu, Z. R., Shen, R. R., Michalke, B., Abbaszade, G., and  
443 Zimmermann, R.: Characteristics of chemical profile, sources and PAH toxicity of PM<sub>2.5</sub> in Beijing in autumn-winter transit  
444 season with regard to domestic heating, pollution control measures and meteorology, *Chemosphere*, 276, doi:  
445 10.1016/j.chemosphere.2021.130143, 2021.

446 Li, W. F., Peng, Y., and Bai, Z. P.: Distributions and sources of n-alkanes in PM<sub>2.5</sub> at urban, industrial and coastal sites in  
447 Tianjin, China, *J. Environ. Sci. (China)*, 22, 1551-1557, doi: 10.1016/S1001-0742(09)60288-6, 2010.

448 Li, X. R., Wang, Y. S., Guo, X. Q., and Wang, Y. F.: Seasonal variation and source apportionment of organic and inorganic  
449 compounds in PM<sub>2.5</sub> and PM<sub>10</sub> particulates in Beijing, China, *J. Environ. Sci. (China)*, 25, 741-750, doi: 10.1016/S1001-  
450 0742(12)60121-1, 2013.

451 Li, Y. S., Cao, J. J., Li, J. J., Zhou, J. M., Xu, H. M., Zhang, R. J., and Ouyang, Z. Y.: Molecular distribution and seasonal  
452 variation of hydrocarbons in PM<sub>2.5</sub> from Beijing during 2006, *Particuology*, 11, 78-85, doi: 10.1016/j.partic.2012.09.002,  
453 2013.

454 Liao, H. T., Lee, C. L., Tsai, W. C., Yu, J. Z., Tsai, S. W., Chou, C. C K, and Wu, C. F.: Source apportionment of urban  
455 PM<sub>2.5</sub> using positive matrix factorization with vertically distributed measurements of trace elements and nonpolar organic  
456 compounds, *Atmos. Pollut. Res.*, 12, 200-207, doi: 10.1016/j.apr.2021.03.007, 2021.

457 Liu, L. Y., Wei, G. L., Wang, J. Z., Guan, Y. F., Wong, C. S, Wu, F. C., and Zeng, E. Y: Anthropogenic activities have  
458 contributed moderately to increased inputs of organic materials in marginal seas off China, *Environ. Sci. Technol.*, 47,  
459 11414-11422, doi: 10.1021/es401751k, 2013.

460 Liu, X. D., Meng, J. J., Hou, Z. F., Yi, Y. N., Wei, B. J., and Fu, M. X.: Pollution Characteristics and Source Analysis of n-  
461 alkanes and Saccharides in PM<sub>2.5</sub> During the Winter in Liaocheng City, *Environ. Sci. (in Chinese)*, 40, 548-557, doi:  
462 10.13227/j.hjlx.201807132, 2019.

463 Lv, L. L., Chen, Y. J., Han, Y., Cui, M., Wei, P., Zheng, M., and Hu, J. N.: High-time-resolution PM<sub>2.5</sub> source apportionment  
464 based on multi-model with organic tracers in Beijing during haze episodes, *Sci. Total Environ.*, 772, 144766, doi:  
465 10.1016/j.scitotenv.2020.144766, 2020.

466 Lyu, R. H., Shi, Z. B., Alam, M. S., Wu, X. F., Liu, D., Vu, T. V, Stark, C., Xu, R. X., Fu, P. Q., Feng, Y. C., and Harrison, R.  
467 M: Alkanes and aliphatic carbonyl compounds in wintertime PM 2.5 in Beijing, China, *Atmos. Environ.*, 202, 244-255, doi:  
468 10.1016/j.atmosenv.2019.01.023, 2019.

469 Lyu, Y., Xu, T. T., Yang, X., Chen, J. M., Cheng, T. T., and Li, X.: Seasonal contributions to size-resolved n-alkanes (C8-  
470 C40) in the Shanghai atmosphere from regional anthropogenic activities and terrestrial plant waxes, *Sci. Total Environ.*, 579,  
471 1918-1928, doi: 10.1016/j.scitotenv.2016.11.201, 2016.

472 Ma, J. Z., Xu, X. B., Zhao, C. S., and Yan, P.: A review of atmospheric chemistry research in China: Photochemical smog,  
473 haze pollution, and gas-aerosol interactions, *Adv. Atmos. Sci.*, 29, 1006-1026, doi: 10.1007/s00376-012-1188-7, 2012.

474 Marzi, R., Torkelson, B. E., and Olson, R. K.: A revised carbon preference index, *Org. Geochem.*, 20, 1303-1306, doi:  
475 10.1016/0146-6380(93)90016-5, 1993.

476 Michoud, V., Kukui, A., Camredon, M., Colomb, A., Bordon, A., Miet, K., Aumont, B., Beekmann, M., Durand-Jolibois, R.,  
477 Perrier, S., Zapf, P., Siour, G., Ait-Helal, w., Locoge, N., Sauvage, S., Afif, C., Gros, V., Furger, M., Ancellet, G., and  
478 Doussin, J. F.: Radical budget analysis in a suburban European site during the MEGAPOLI summer field campaign, *Atmos.*  
479 *Chem. Phys.*, 12, 11951-11974, doi: 10.5194/acp-12-11951-2012, 2012.

480 Moeinaddini, M., Sari, A. E., Bakhtiari, A. R., Chan, A. Y. C., Taghavi, S. M., Hawker, D., and Connell, D.: Source  
481 apportionment of PAHs and n-alkanes in respirable particles in Tehran, Iran by wind sector and vertical profile, *Environ. Sci.*  
482 *Pollut. Res.*, 21, 7757-7772, doi: 10.1007/s11356-014-2694-1, 2014.

483 Niu, H. Y., Zhao, X., Dai, Z. X., Wang, G. H., and Wang, L. S.: Characterization, source apportionment of particulate matter  
484 and n-alkanes in atmospheric aerosols in Nanjing City, *Environ. pollut. Control (in Chinese)*, 27, 363-366, doi:  
485 10.1007/s10971-005-6694-y, 2005.

486 Oros, D. R., and Simoneit, B. R. T.: Identification and emission rates of molecular tracers in coal smoke particulate matter,  
487 *Fuel*, 79, 515-536, doi: 10.1016/S0016-2361(99)00153-2, 2000.

488 Presto, A. A., Miracolo, M. A., Kroll, J. H., Worsnop, D. R., Robinson, A. L., and Donahue, N. M.: Intermediate-volatility  
489 organic compounds: a potential source of ambient oxidized organic aerosol, *Environ. Sci. Technol.*, 43, 4744-4749, doi:  
490 10.1021/es803219q, 2009.

491 Qi, M. X., Jiang, L., Liu, Y. X., Xiong, Q. L., Sun, C. Y., Li, X., Zhao, W. J., and Yang, X. C.: Analysis of the Characteristics  
492 and Sources of Carbonaceous Aerosols in PM<sub>2.5</sub> in the Beijing, Tianjin, and Langfang Region, China, *Int. J. Environ. Res.*  
493 *Public Health*, 15, 1438, doi: 10.3390/ijerph15071483, 2018.

494 Ren, L. J., Fu, P. Q., He, Y., Hou, J. Z., Chen, J., Pavuluri, C. M., Sun, Y. L., and Wang, Z. F.: Molecular distributions and  
495 compound-specific stable carbon isotopic compositions of lipids in wintertime aerosols from Beijing, *Sci. Rep.*, 6, 27481,  
496 doi: 10.1038/srep27481, 2016.

497 Ren, L. J., Hu, W., Hou, J. Z., Li, L. J., Yue, S. Y., Sun, Y. L., Wang, Z. F., Li, X. F., Pavuluri, C. M., Hou, S. J., Liu, C. Q.,  
498 Kawamura, K., Ellam, R. M., and Fu, P. Q.: Compound-Specific Stable Carbon Isotope Ratios of Terrestrial Biomarkers in  
499 Urban Aerosols from Beijing, China, *ACS Earth Space Chem.*, 3, 1896-1904, doi: 10.1021/acsearthspacechem.9b00113,  
500 2019.

501 Ren, Y. Q., Wang, G. H., Wu, C., Wang, J. Y., Li, J. J., Zhang, L., Han, Y. N., Liu, L., Cao, C., Cao, J. J., He, Q., and Liu, X.  
502 C.: Changes in concentration, composition and source contribution of atmospheric organic aerosols by shifting coal to  
503 natural gas in Urumqi, *Atmos. Environ.*, 148, 306-315, doi: 10.1016/j.atmosenv.2016.10.053, 2017.

504 Rogge, W. F., Hildemann, L. M., Mazurek, M. A., Cass, G. R., and Simoneit, B. R. T.: Sources of fine organic aerosol. 4.  
505 Particulate abrasion products from leaf surfaces of urban plants, *Environ. Sci. Technol.*, 27, 2700-2711, doi:  
506 10.1021/es00049a008, 1993.

507 Schauer, J. J., Kleeman, M. J., Cass, G. R., and Simoneit, B. R. T.: Measurement of Emissions from Air Pollution Sources. 5.  
508 C1-C32 Organic Compounds from gasoline-Powered Motor Vehicles, *Environ. Sci. Technol.*, 36, 1169-1180, doi:  
509 10.1021/es0108077, 2002.

510 Simoneit, B. R. T.: Application of Molecular Marker Analysis to Vehicular Exhaust for Source Reconciliations, *Int. J. Environ.*  
511 *Anal. Chem.*, 22, 203-232, doi: 10.1080/03067318508076422, 1985.

512 Simoneit, B. R T: Organic matter of the troposphere - V: Application of molecular marker analysis to biogenic emissions into  
513 the troposphere for source reconciliations, *J. Atmos. Chem.*, 8, 251-275, doi: 10.1007/BF00051497, 1989.

514 Simoneit, B. R T, Kobayashi, M., Mochida, M., Kawamura, K., and Huebert, B. J: Aerosol particles collected on aircraft  
515 flights over the northwestern Pacific region during the ACE-Asia campaign: composition and major sources of the organic  
516 compounds, *J. Geophys. Res.*, 109, doi: 10.1029/2004JD004565, 2004.

517 Sun, N., Li, X. D., Ji, Y., Huang, H. Y., Ye, Z. L., and Zhao, Z. Z.: Sources of PM<sub>2.5</sub>-Associated PAHs and n-alkanes in  
518 Changzhou China, *Atmosphere*, 12, 1127, doi: 10.3390/atmos12091127, 2021.

519 Tang, G. Q., Zhang, J. Q., Zhu, X. W., Song, T., and Wang, Y. S.: Mixing layer height and its implications for air pollution  
520 over Beijing, China, *Atmospheric Chem. Phys.*, 16, 2459-2475, doi: 10.5194/acpd-15-28249-2015, 2016.

521 US EPA: EPA Positive Matrix Factorization (PMF) 5.0 Fundamentals and User Guide. EPA/600/R-14/108, EPA, Washington,  
522 DC, 2014.

523 Wagner, P., and Schäfer, K.: Influence of mixing layer height on air pollutant concentrations in an urban street canyon, *Urban*  
524 *Clim.*, 22, 64-79, doi: 10.1016/j.uclim.2015.11.001, 2017.

525 Wang, F. W., Guo, Z. G., Lin, T., and Rose, N. L: Seasonal variation of carbonaceous pollutants in PM<sub>2.5</sub> at an urban  
526 'supersite' in Shanghai, China, *Chemosphere*, 146, 238-244, doi: 10.1016/j.chemosphere.2015.12.036, 2016.

527 Wang, G. H., and Kawamura, K.: Molecular characteristics of urban organic aerosols from Nanjing: a case study of a mega-  
528 city in China, *Environ. Sci. Technol.*, 39, 7430-7438, doi: 10.1021/es051055+, 2005.

529 Wang, G. H., Kawamura, K., Lee, S. C., Ho, K. F., and Cao, J. J.: Molecular, Seasonal, and Spatial Distributions of Organic  
530 Aerosols from Fourteen Chinese Cities, *Environ. Sci. Technol.*, 40, 4619-4625, doi: 10.1021/es060291x, 2006.

531 Wang, G. H., Huang, L. M., Zhao, X., Niu, H. Y., and Dai, Z. X.: Aliphatic and polycyclic aromatic hydrocarbons of  
532 atmospheric aerosols in five locations of Nanjing urban area, China, *Atmos. Res.*, 81, 54-66, doi:  
533 10.1016/j.atmosres.2005.11.004, 2006.

534 Wang, G. H., Zhang, R. Y., Gomez, M. E., Yang, L. X., Zamora, M. L., Hu, M., Lin, Y., Peng, J. F., Guo, S., Meng, J. J., Li, J.  
535 J., Chen, C. L., Hu, T. F., Ren, Y. Q., Wang, Y. S., Gao, J., Cao, J. J., An, Z. S., Zhou, W. J., Li, G. H., Wang, J. Y., Tian, P. F.,  
536 Marrero-Ortiz, W., Secrest, J., Du, Z. F., Zheng, J., Shang, D. J., Zheng, L. M., Shao, M., Wang, W. G., Huang, Y., Wang, Y.,  
537 Zhu, Y. J., Li, Y. X., Hu, J. X., Pan, B. W., Cai, L., Cheng, Y. T., Ji, Y. M., Zhang, F., Rosenfeld, D., Liss, P. S., Duce, R. A.,  
538 Kolb, C. E., and Molina, M. J: Persistent sulfate formation from London Fog to China haze, *P. Natl. Acad. Sci. USA*, 113,  
539 13630-13635, doi: 10.1073/pnas.1616540113, 2016.

540 Wang, H. F., Li, Z. Q., Lv, Y., Zhang, Y., Xu, H., Guo, J. P., and Goloub, P.: Determination and climatology of the diurnal  
541 cycle of the atmospheric mixing layer height over Beijing 2013–2018: lidar measurements and implications for air pollution,  
542 *Atmospheric Chem. Phys.*, 20, 8839-8854, doi: 10.5194/acp-20-8839-2020, 2020.

543 Wang, J. Z., Ho, S. S. H., Ma, S. X., Cao, J. J., Dai, W. T., Liu, S. X., Shen, Z. X., Huang, R. J., Wang, G. H., and Han, Y. M.:  
544 Carbonaceous species in PM<sub>2.5</sub> and PM<sub>10</sub> in urban area of Zhengzhou in China: Seasonal variations and source  
545 apportionment, *Sci. Total Environ.*, 550, 961-971, doi: 10.1016/j.scitotenv.2016.01.138, 2016.

546 Wang, Q., Jiang, N., Yin, S. S., Li, X., Yu, F., Guo, Y., and Zhang, R. Q.: Carbonaceous species in PM<sub>2.5</sub> and PM<sub>10</sub> in urban  
547 area of Zhengzhou in China: Seasonal variations and source apportionment, *Atmos. Res.*, 191, 1-11, doi:  
548 10.1016/j.atmosres.2017.02.003, 2017.

549 Wei, M., Li, M. Y., Xu, C. H., Xu, P. J., and Liu, H. F.: Pollution characteristics of bioaerosols in PM<sub>2.5</sub> during the winter  
550 heating season in a coastal city of northern China, *Environ. Sci. Pollut. Res.*, 27, 27750-27761, doi: 10.1007/s11356-020-  
551 09070-y, 2020.

552 Wick, C. D., Siepmann, J., Klotz, W. L., and Schure, M. R.: Temperature effects on the retention of n-alkanes and arenes in  
553 helium–squalane gas–liquid chromatography: experiment and molecular simulation, *J. Chromatogr. A*, 957, 181-190, doi:

554 10.1016/S0021-9673(02)00171-1, 2002.

555 Xu, H. M., Tao, J., Ho, S. S. H., Ho, K. F., Cao, J. J., Li, N., Chow, J. C., Wang, G. H., Han, Y. M., and Zhang, R. J.:  
556 Characteristics of fine particulate non-polar organic compounds in Guangzhou during the 16th Asian Games: Effectiveness  
557 of air pollution controls, *Atmos. Environ.*, 76, 94-101, doi: 10.1016/j.atmosenv.2012.12.037, 2013.

558 Xu, T. T., Lv, Y., Cheng, T. T., and Li, X.: Using comprehensive GC×GC to study PAHs and n-alkanes associated with  
559 PM<sub>2.5</sub> in urban atmosphere, *Environ. Sci. Pollut. Res.*, 22, 5253-5262, doi: 10.1007/s11356-014-3695-9, 2015.

560 Yadav, S., Tandon, A., and Attri, A., Monthly and seasonal variation in aerosol associated n-alkane profiles in relation to  
561 meteorological parameters in New Delhi, India, *Aerosol Air Qual. Res.*, 13, 287-300, doi: 10.4209/aaqr.2012.01.0004, 2013.

562 Yang, X. H., Luo, F. X., Li, J. Q., Chen, D. Y., E, Y., Lin, W. L., and Jin, J.: Alkyl and aromatic nitrates in atmospheric  
563 particles determined by gas chromatography tandem mass spectrometry, *J. Am. Soc. Mass Spectrom.*, 30, 2762-2770, doi:  
564 10.1007/s13361-019-02347-8, 2019.

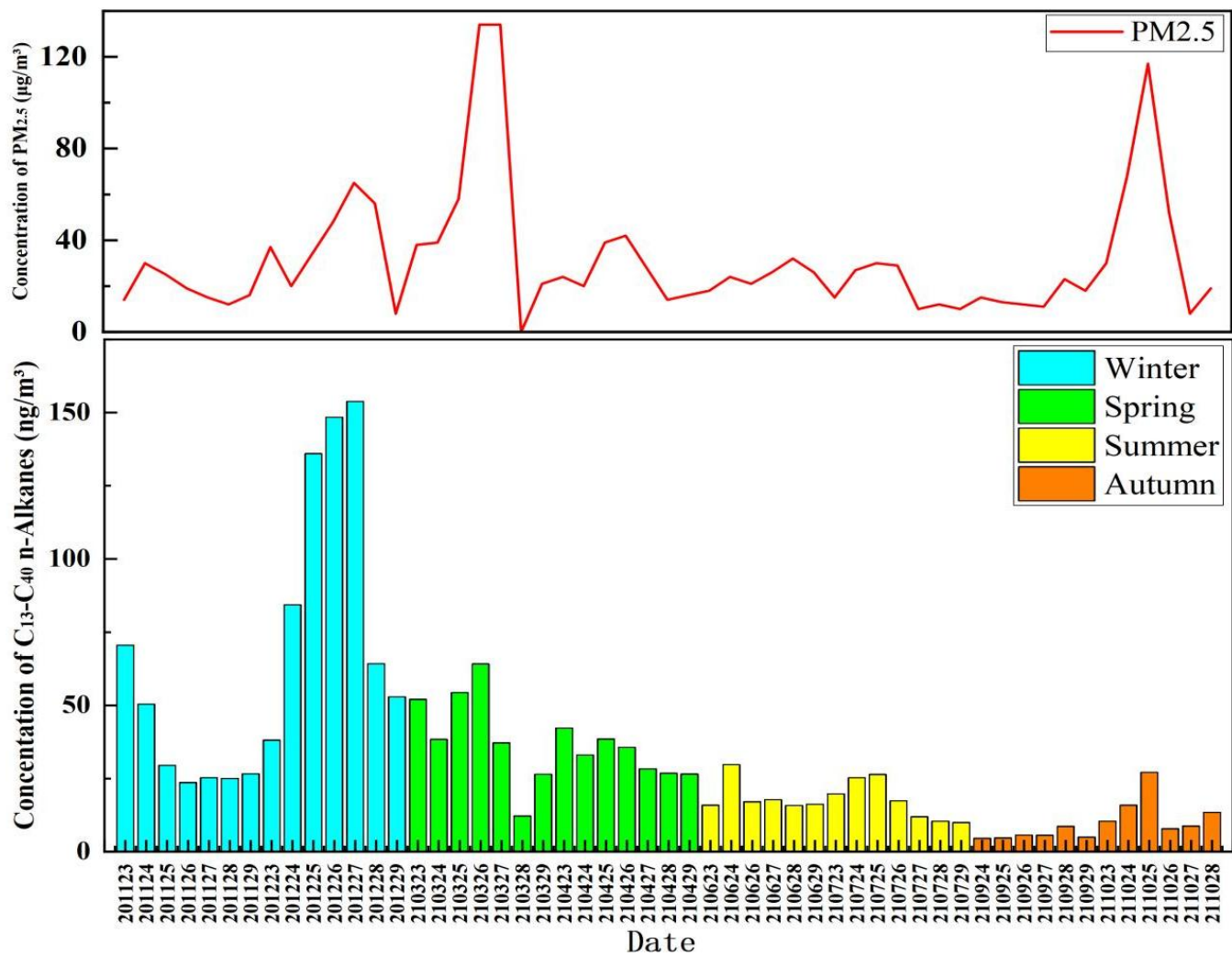
565 Yao, L., Li, X. R., Guo, X. Q., Liu, X. R., and Wang, Y. S.: Pollution Characteristics of n-alkanes in Atmospheric Fine  
566 Particles During Spring Festival of 2007 in Beijing, *Environ. Sci. (in Chinese)*, 30, 589-593, doi:  
567 10.13227/j.hjlx.2009.02.042, 2009.

568 Yuan, J. W., Liu, G., Li, J. H., and Xu, H.: Chemical Composition of Alkanes and Organic Acids in Vehicle Exhaust, *Environ.*  
569 *Sci. (in Chinese)*, 37, 2052-2058, doi: 10.13227/j.hjlx.2016.06.007, 2016.

570 Zhao, Y., Zhang, Y., Fu, P., Ho, S. S., Ho, K. F., Liu, F., Zou, S., Wang, S., and Lai, S.: Non-polar organic compounds in  
571 marine aerosols over the northern South China Sea: Influence of continental outflow, *Chemosphere*, 153, 332-339, doi:  
572 10.1016/j.chemosphere.2016.03.069, 2016.

573 Zhang, R. Y., Wang, G. H., Guo, S., Zamora, M. L., Ying, Q., Lin, Y., Wang, W. G., Hu, M., and Wang, Y.: Formation of  
574 urban fine particulate matter, *Chem. Rev.*, 115, 3803-3855, doi: 10.1021/acs.chemrev.5b00067, 2015.

575 Zhu, X. L., Zhang, Y. H., Zeng, L. M., and Wang, W.: Source Identification of Ambient PM<sub>2.5</sub> in Beijing, *Res. Environ. Sci.*  
576 (in Chinese), 18, 1-5, doi: 10.1007/s10971-005-6694-y, 2005.



577

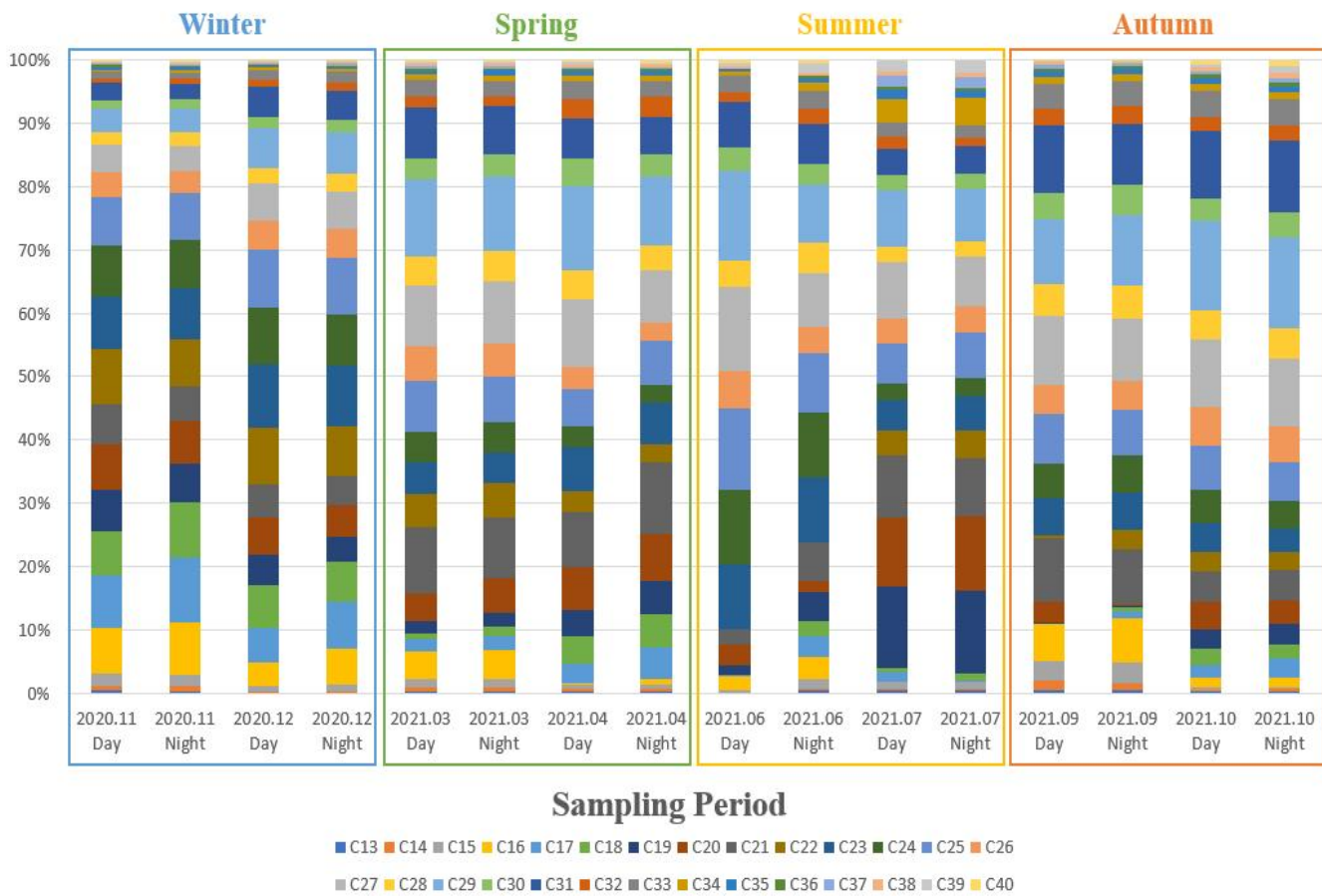
578

Figure 1. Temporal variations in PM<sub>2.5</sub> and particulate-bound *n*-alkane concentrations during the sampling period in Beijing.

579

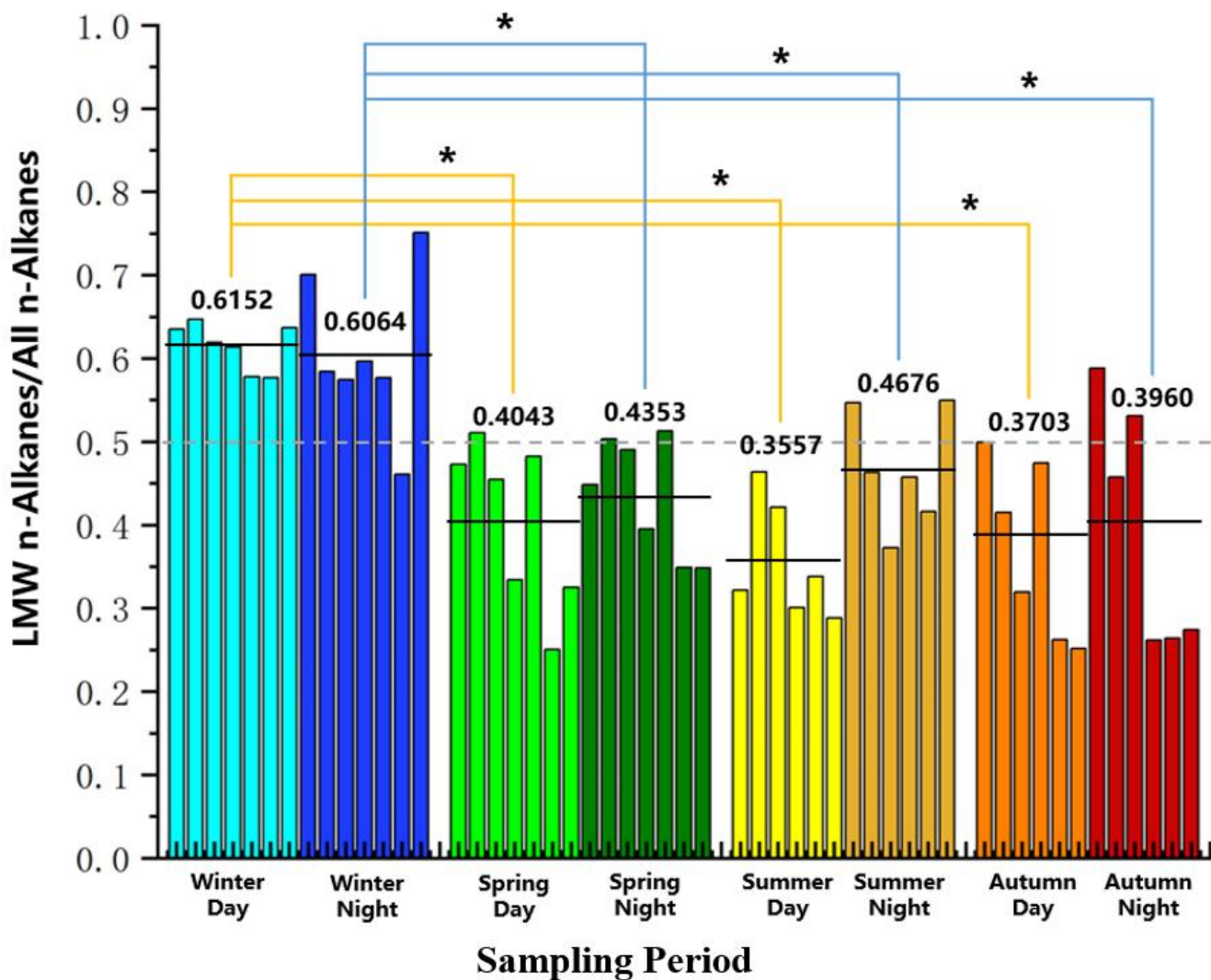
(The concentrations of C<sub>13</sub>-C<sub>40</sub> *n*-Alkanes and PM<sub>2.5</sub> are the average of the day and night).





580

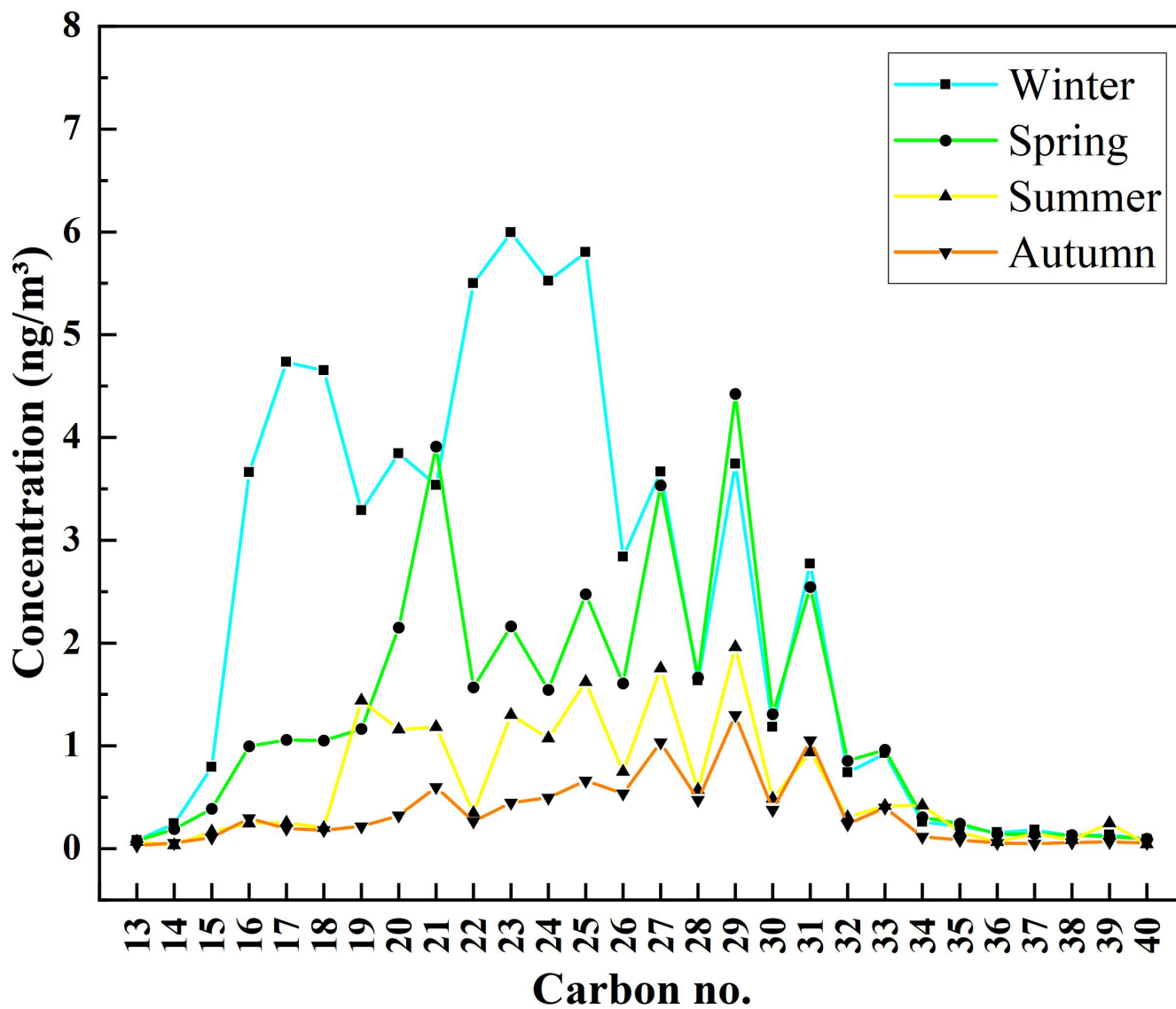
581 **Figure 2. Contributions of particulate-bound *n*-alkane homologs to the total *n*-alkane concentrations in the day and night samples**  
 582 **in the different seasons of Beijing.**



583

584 Figure 3. Contributions of low molecular weight *n*-alkanes in the day and night samples in the different seasons of Beijing.

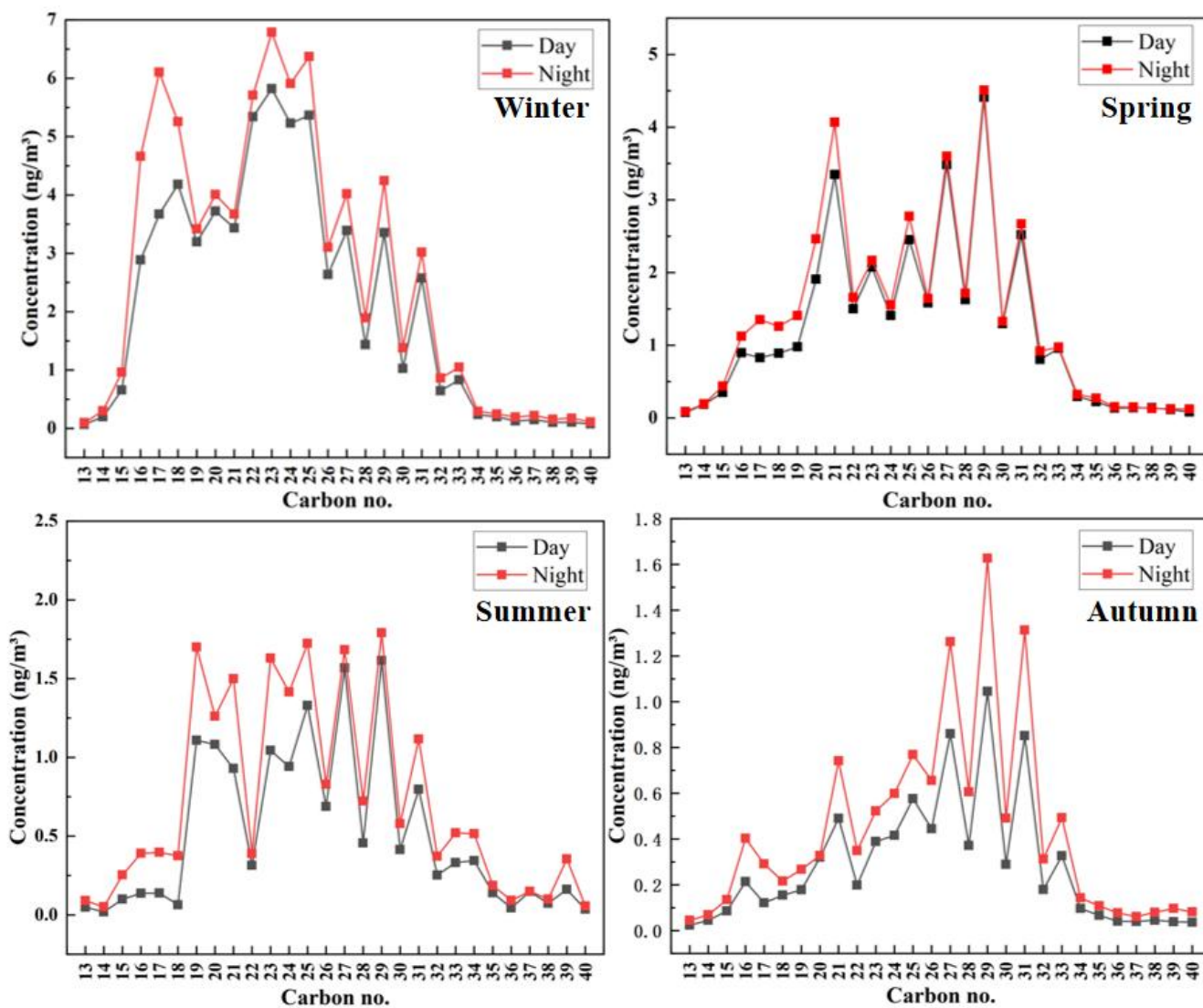
585 (\* indicates a significant difference, dashed line represents the 50% percentage, solid line shows the average proportion of LMW  
 586 *n*-alkanes).



587

588

Figure 4. Average concentration distributions of the particulate-bound *n*-alkane homologs in the different seasons of Beijing.

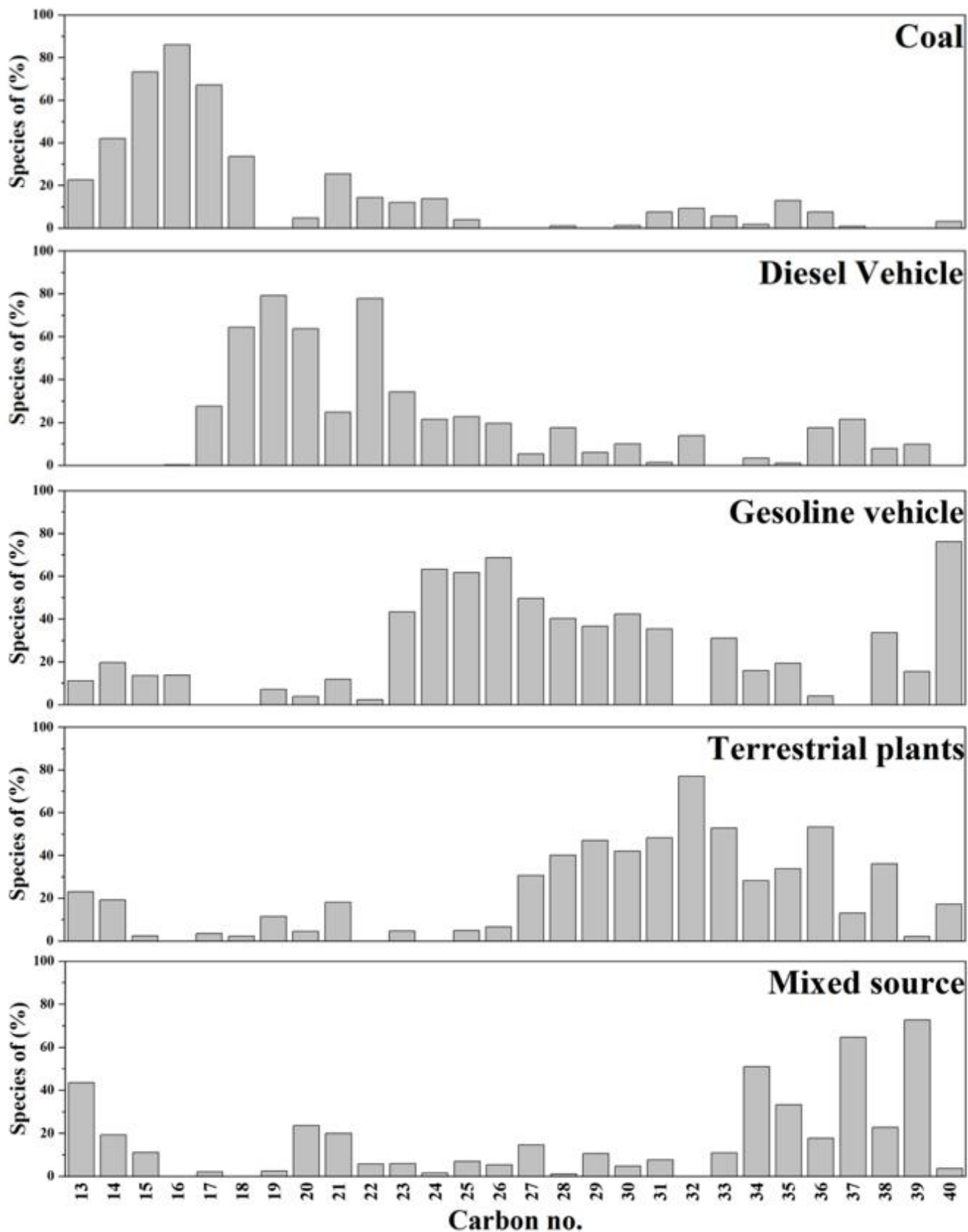


589

590

591

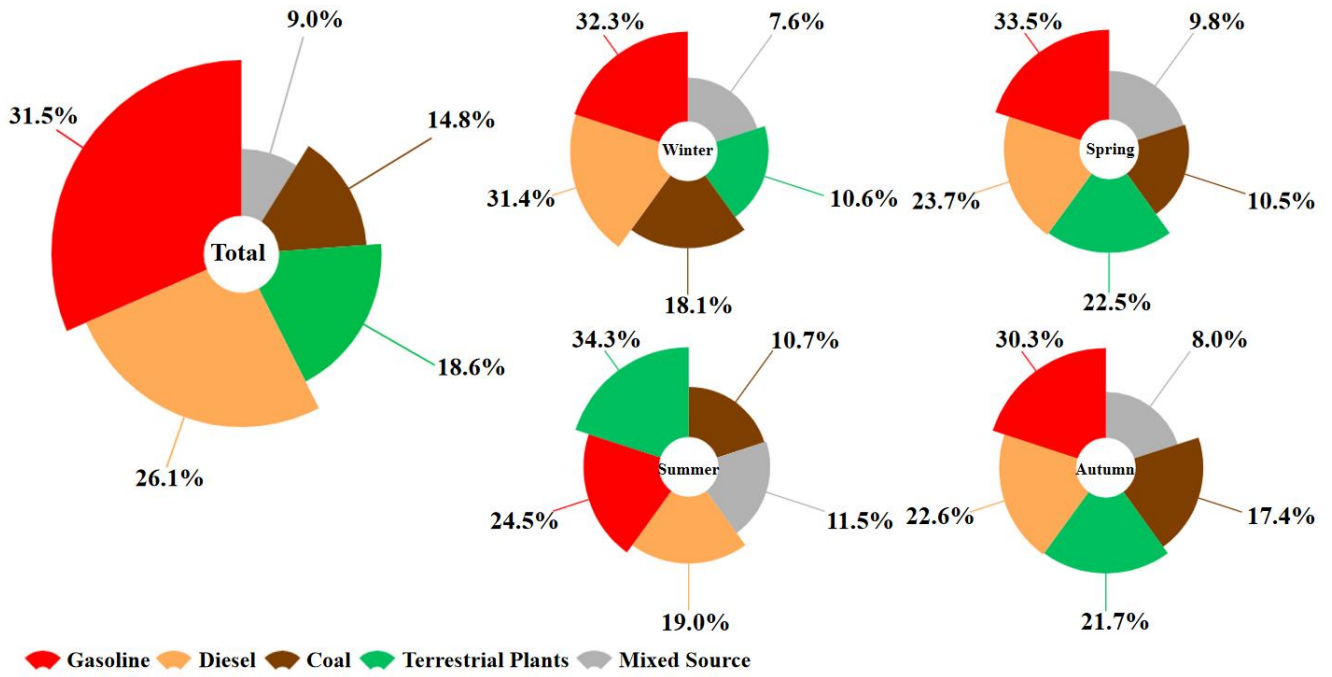
Figure 5. Concentration distributions of the particulate-bound *n*-alkane homologs in the day and night in the different seasons of Beijing.



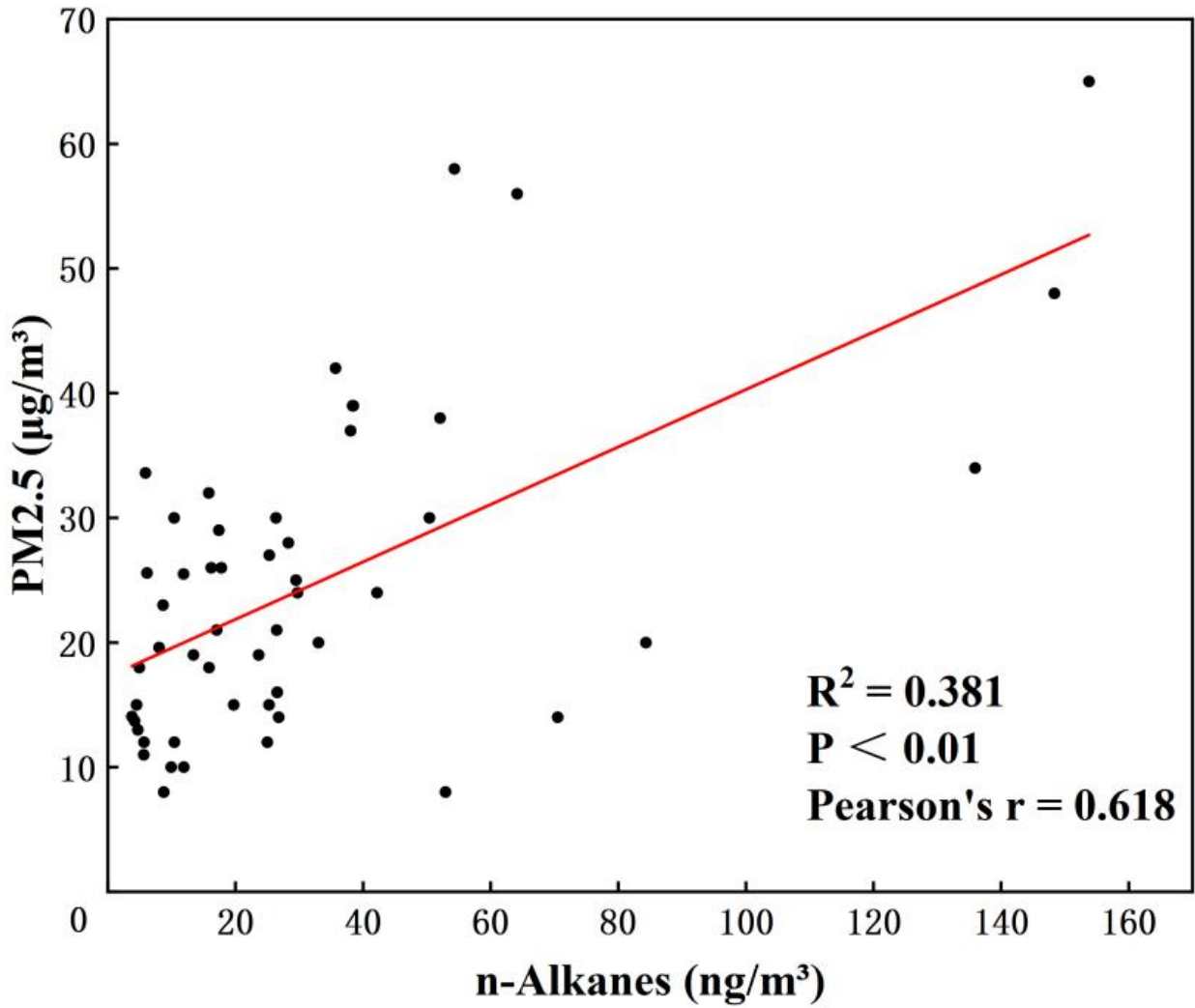
592

593

Figure 6. Proportions of the different *n*-alkane homologs in the factors identified by the positive matrix factorization model.



594  
595 Figure 7. Sources and contributions of particulate-bound *n*-alkanes in Beijing.



596  
597 Figure 8. Association between particulate-bound *n*-alkanes and PM2.5 in Beijing.

598 **Table 1. PM2.5 and particulate-bound *n*-alkane concentrations in different seasons in Beijing.**

Species	Winter <sup>a</sup>		Spring <sup>b</sup>		Summer <sup>c</sup>		Fall <sup>d</sup>	
	Mean	Range	Mean	Range	Mean	Range	Mean	Range
PM2.5 ( $\mu\text{g}/\text{m}^3$ )	28.5	8.00–65.0	43.5	0–134	21.5	10.0–32.0	32.2	8.00–117
<i>n</i> -Alkanes ( $\text{ng}/\text{m}^3$ )	66.3	17.1–89.9	36.8	12.2–64.1	18.0	9.92–29.7	9.78	4.51–27.1

599 <sup>a</sup> Winter: November and December in 2020;600 <sup>b</sup> Spring: March and April in 2021;601 <sup>c</sup> Summer: June and July in 2021;602 <sup>d</sup> Fall: September and October in 2021.603 **Table 2. Source indices for particulate-bound *n*-alkane in Beijing.**

Source Index	Winter		Spring		Summer		Fall	
	Day	Night	Day	Night	Day	Night	Day	Night
<b>Cmax<sup>a</sup></b>	C23	C23	C29	C29	C29	C29	C29	C29
<b>CPI<sup>b</sup></b>	1.16	1.18	1.85	1.76	2.15	1.87	1.90	1.78
<b>WNA%<sup>c</sup></b>	17.4	18.5	35.0	33.1	43.0	39.2	39.6	35.1
<b>PNA%<sup>d</sup></b>	82.6	81.5	65.0	66.9	57.0	60.8	60.5	64.9

604 <sup>a</sup> Cmax: Carbon maximum number;605 <sup>b</sup> CPI: Carbon preference index;606 <sup>c</sup> WNA%: Plant wax *n*-alkane ratio;607 <sup>d</sup> PNA%: Petrogenic *n*-alkane ratio.